Am J Physiol Cell Physiol 318: C360–C371, 2020.
First published November 27, 2019; doi:10.1152/ajpcell.00180.2019.

RESEARCH ARTICLE

The pleiotropic molecule NGF regulates the in vitro properties of fibroblasts, keratinocytes, and endothelial cells: implications for wound healing

N. Gostynska,[1]* M. Pannella,[1]* M. L. Rocco,[3] L. Giardino,[1,2] L. Aloe,[3] and L. Calzà[1,4]

[1]*Health Sciences and Technologies-Interdepartmental Center for Industrial Research, University of Bologna, Ozzano dell'Emilia, Italy;* [2]*Department of Veterinary Medical Sciences, University of Bologna, Ozzano dell'Emilia, Italy;* [3]*IRET Foundation, Ozzano dell'Emilia, Italy; and* [4]*Department of Pharmacy and Biotechnology, University of Bologna, Ozzano dell'Emilia, Italy*

Submitted 29 May 2019; accepted in final form 20 November 2019

Gostynska N, Pannella M, Rocco ML, Giardino L, Aloe L, Calzà L. The pleiotropic molecule NGF regulates the in vitro properties of fibroblasts, keratinocytes, and endothelial cells: implications for wound healing. *Am J Physiol Cell Physiol* 318: C360–C371, 2020. First published November 27, 2019; doi: 10.1152/ajpcell.00180.2019.—Nerve growth factor (NGF) is recognized as a pleiotropic molecule, exerting a variety of biological effects on different cell types and pathophysiological conditions, and its role in tissue wound healing has been recently highlighted. However, the preferential cellular target of NGF is still elusive in the complex cellular and molecular cross talk that accompanies wound healing. Thus, to explore possible NGF cellular targets in skin wound healing, we investigated the in vitro NGF responsiveness of keratinocytes (cell line HEKa), fibroblasts (cell line BJ), and endothelial cells (cell line HUVEC), also in the presence of adverse microenvironmental conditions, e.g., hyperglycemia. The main results are summarized as follows: *1*) NGF stimulates keratinocyte proliferation and HUVEC proliferation and angiogenesis in a dose-dependent manner although it has no effect on fibroblast proliferation; *2*) NGF stimulates keratinocyte but not fibroblast migration in the wound healing assay; and *3*) NGF completely reverts the proliferation impairment of keratinocytes and the angiogenesis impairment of HUVECs induced by high D-glucose concentration in the culture medium. These results contribute to better understanding possible targets for the therapeutic use of NGF in skin repair.

angiogenesis; cell migration; NGF; wound healing

INTRODUCTION

Nerve growth factor (NGF) is a molecule originally described as "neurotrophic factor" by Rita Levi-Montalcini. However, several decades of scientific research have shown that many cell types produce NGF and/or express NGF receptors; thus, NGF has been reconsidered as a "pleiotropic molecule" that regulates various physiological and pathological processes, such as inflammation, immunity, skin and mucosa turnover and repair, angiogenesis, etc. (3, 21).

In particular, endogenous NGF has been shown to play a role in skin and mucosal wound healing, demonstrated in various animal and lesion models as well as human pathologies (8, 24). Several of the cellular actors involved in epithelial tissue repair are NGF-producing or NGF-dependent cells, expressing the tropomyosin receptor kinase A (TrkA) high-affinity receptor. For example, TrkA is expressed by basal keratinocytes in human skin (29), and in dermal fibroblasts and myofibroblasts (38), whereas NGF has been observed in esophageal keratinocyte progenitor cells (43) and is expressed in dermal fibroblasts (38). NGF has been also indicated as a novel angiogenic molecule that exerts a variety of effects on endothelial cells by way of autocrine and/or paracrine mechanisms (5, 36). Inflammatory and immune cells also express NGF high (TrkA)- and low (p75)-affinity receptors (32). Finally, the thinly myelinated Aδ- or unmyelinated C-fibers that innervate the skin (dermis and epidermis) are dependent on the NGF-TrkA system during development (16).

A number of observations also suggest that pathological states modify the NGF-TrkA system in several cell types and tissues. In particular, inflammation can greatly enhance the synthesis of NGF in the tissues, and in vitro and in vivo evidence indicates that inflammatory cytokines induce or enhance NGF synthesis in a variety of cells, such as fibroblasts and epithelial, endothelial, glial, neuronal, and immune cells (32). On the other hand, an impairment in endogenous NGF synthesis has been implicated in delayed wound repair, for example, in diabetic rats (2).

Taking this evidence as a starting point, the topical application of NGF has been considered as possible therapy to accelerate wound repair in pathological conditions characterized by an impaired healing process (24), and several reports have described the positive effect of NGF in epithelial wound healing, including chronic nonhealing cutaneous ulcers in diabetic rodents (53). Moreover, the positive effect of NGF on corneal healing described since 2000 (19) has led to Food and Drug Administration (FDA) approval of NGF ocular drops for the treatment of rare neurotrophic keratitis.

However, wound repair is a complex phenomenon involving numerous cell types in a defined temporal sequence, and it is not currently clear which cell type preferentially responds to endogenous or exogenous NGF availability in normal and pathological conditions. To examine these aspects, we investigated the effect of NGF on three pivotal cell types involved in skin wound healing (keratinocytes, fibroblasts, and endothelial cells) in terms of NGF receptor regulation, proliferation, and migration, also in the presence of high glucose concentrations in vitro. The choice of the cell systems has been directed to the use of cell lines widely used for drug screening. Mouse

* N. Gostynska and M. Pannella contributed equally to this work.

Address for reprint requests and other correspondence: L. Calzà, CIRI-SDV, University of Bologna, Via Tolara di Sopra 41/E, 40064 Ozzano dell'Emilia (BO), Italy (e-mail: laura.calza@unibo.it).

NGF (mNGF) was used in this study, since it has a high number of amino acid sequences identical to human NGF (90%), and the NGF preparation used in this study has proven effective in human tissues, for example, in promoting wound healing in diabetic patients (12) and in human corneal lesions (21, 22).

MATERIALS AND METHODS

Cell cultures. The human skin fibroblast cell line BJ was purchased from the American Type Culture Collection (CRL-2522; ATCC, Manassas, VA). This cell line was generated from newborn normal male human foreskin. According to the ATCC indications, these cells have a reported normal diploid karyotype at population doubling 61 but an abnormal karyotype at population doubling 82. They are telomerase negative. Cells were cultured under standard conditions, in minimum essential medium (MEM; Gibco, Waltham, MA) containing 5.5 mM D-glucose, supplemented with 10% heat-inactivated fetal bovine serum (FBS; Thermo Fisher Scientific, Waltham, MA) and 1% penicillin (100 U/ml)-streptomycin (100 μg/ml); Thermo Fisher Scientific), in a humidified incubator of 5% CO_2 at 37°C. When 70–80% confluency was reached, cells were passaged by trypsinization and subcultured in 75-cm^2 flasks. At initial seeding, the cell density was between 7×10^3 and 10×10^3 cells/cm^2.

The normal adult human primary epidermal keratinocyte cell line HEKa was purchased from the American Type Culture Collection (ATCC PCS-200–011). Cells were grown in dermal cell basal media (ATCC PCS-200–030) supplemented with Keratinocyte Growth Kit components (ATCC PCS-200–040) containing the following growth components: 0.4% bovine pituitary extract (BPE), 0.1% recombinant human (rh) TGF-α (0.5 ng/mL), 3% L-glutamine (6 mM), 0.1% hydrocortisone hemisuccinate (100 ng/mL), 0.1% rh insulin (5 mg/mL), 0.1% epinephrine (1.0 mM), 0.1% apotransferrin (5 mg/mL; ATCC PCS-200–400), and 0.1% penicillin (100 U/ml)-streptomycin (100 μg/ml; Thermo Fisher Scientific), in a humidified incubator of 5% CO_2 at 37°C. When 70–80% confluency was reached, cells were passaged by trypsinization and trypsin-neutralizing solution and subcultured in 75-cm^2 flasks. At initial seeding, the cell density was between 5×10^3 and 8×10^3 cells/cm^2.

Primary human umbilical vein endothelial cells pooled (HUVECp) were purchased from Gibco (cell culture catalog no. C-015–5C; Invitrogen, Waltham, MA). These cells were pooled from multiple isolates. Cells were grown in phenol red-free basal medium M200 (Life Technologies, Waltham, MA) containing 10% FBS (Life Technologies), 1% penicillin-streptomycin, 1% L-glutamine, and growth factors (low-serum growth supplement; Life Technologies) supplemented with low-serum growth supplement containing the following growth components: 2% vol/vol FBS; 1 μg/mL hydrocortisone, 10 ng/mL human epidermal growth factor, 3 ng/mL basic fibroblast growth factor, and 10 μg/mL heparin in a humidified incubator of 5% CO_2 at 37°C. When 70–80% confluency was reached, cells were passaged by trypsinization and trypsin-neutralizing solution and subcultured in 75-cm^2 flasks. At initial seeding, the cell density was 7.5×10^3 cells/cm^2.

NGF and anti-NGF antibody preparation. Murine β-NGF was purified in our laboratory from adult male mouse submaxillary glands (4), with minor revisions. The anti-NGF antibody was raised in goat and purified following an established procedure (51). Male Crl: CD1(ICR) mice, 6–8 mo old, were obtained from Charles River Italia and euthanized by cervical translocation.

All animal protocols described here were carried out according to the European Community Council Directives 86/609/EEC, approved by the Italian Ministry of Health, and the European Community Council Directives 2010/63/UE. Moreover, animal protocols were carried out in compliance with the guidelines published in the Animal Research: Reporting In Vivo Experiments and National Institutes of Health *Guide for the Care and Use of Laboratory Animals*.

Cell proliferation. Cells were seeded in a 96-well plate at a density of 3.5×10^3 cells/well for fibroblasts in their cell culture medium with a lower amount of FBS (2%), at 2.0×10^3 cells/well for keratinocytes in their culture medium without FBS, and at 2.0×10^3 cells/well for HUVECs in their complete culture medium. Cells were then treated with different concentrations of mNGF (0, 50, 100, and 200 ng/mL). On every 2nd day from *days 0* to *8*, cells were detached by trypsinization and counted using a hemocytometer. Cells from three wells per group were counted, and each well was counted two times, taking all nine squares in the hemocytometer into account. The medium was changed every 2 days, and new NGF was added.

Tube formation assay. HUVECs were seeded in a 24-well plate at a density of 9×10^4 cells/well on gelatin coating in a culture medium containing mNGF (50, 100, and 200 ng/mL) overnight in a humidified incubator of 5% CO_2 at 37°C. The next day, cells were detached using trypsin EDTA and seeded on Geltrex LDEV-free matrix (Thermo Fisher Scientific, Waltham, MA) in the culture medium with mNGF (50, 100, and 200 ng/mL) for the tube formation assay. The assay was blocked after 8 h, this being the time of maximum tube net extension under the experimental conditions used.

Immunostaining. Indirect immunofluorescence was used to identify $trkA^{NGFR}$ high- and $p75^{NTR}$ low-affinity NGF receptors, to characterize the cell lines, and to analyze the proliferation also after mNGF stimulation. In each cell line, NGF-treated and untreated cultures were processed in the same experimental session. Cells were seeded on cover slips at the density of 2×10^4 cells/well for fibroblasts, 6×10^4 cells/well for keratinocytes, and 6×10^4 cells/well for HUVECs. Cells were grown in their cell culture medium without FBS (keratinocytes), with 2% of FBS (fibroblasts), or in complete medium (HUVEC) in the presence or absence of 200 ng/mL of mNGF. After 5 days of culture, cells were fixed with 4% paraformaldehyde, and the following primary antibodies were used: 1:500 rabbit anti-TrkA (Abcam, Cambridge, UK), 1:500 rabbit anti-p75 (Promega, Madison, WI), and 1:100 mouse anti-vimentin (Santa Cruz Biotechnology, Dallas, TX) to characterize fibroblasts; 1:200 mouse anti-platelet/endothelial cell adhesion molecule-1 (PECAM1; Santa Cruz Biotechnology); and 1:150 rabbit anti-VE cadherin (Thermo Fisher, Waltham, MA) to characterize HUVECs; 1:100 guinea pig anti-keratin (Sigma-Aldrich, Burlington, MA) and 1:200 rabbit anti-laminin (Sigma-Aldrich) to characterize keratinocytes; and 1:200 goat anti-minichromosome maintenance complex component 2 (MCM2, N-19; Santa Cruz, Biotechnology) to evaluate cell proliferation in all cell lines. Donkey rhodamine red-conjugated anti-rabbit (Jackson Laboratories), donkey Alexa 488-conjugated anti-mouse (Thermo Fisher), donkey rhodamine red-conjugated anti-goat (Jackson Laboratories), and donkey Cy^{th} 2 conjugated anti-guinea pig (Jackson Laboratories) were used as secondary antibodies. All primary antisera have been extensively used in the scientific literature. Control experiments were carried out by using the secondary antiserum, alone, and all staining to compare was performed in the same experimental session.

After immunofluorescence staining, cells were incubated with the nuclear dye Hoechst 33258 (1 μg/mL in PBS and 0.3% Triton X-100) for 20 min at room temperature. Cells were finally washed in PBS and mounted in glycerol and PBS (3:1 vol/vol) containing 0.1% paraphenylenediamine.

Wound assay. Fibroblasts (60×10^3 cells/well) and keratinocytes (6×10^4 cells/well) were seeded in a 24-well plate, using 3 wells/group, and grown in their complete cell culture medium until they reached a confluent monolayer. The cells were then pretreated with different concentrations of mNGF (0, 50, 100, and 200 ng/mL) or mNGF (200 ng/mL) with anti-NGF antibodies (10 μg/mL, neutralization experiments) in cell culture medium without FBS for 16 h. Next, the linear scratch through the middle of each well was produced using a sterile pipette tip (200 μL), and the medium was replaced with or without NGF/anti-NGF antibodies. Images of the wounded cell monolayers were taken after 10 h using an optic microscope (IX70;

Olympus), the area of the wound was measured using ImageJ software, and the percentage of wound closure was calculated.

Glucose treatment and wound assay. Fibroblasts were seeded in a 24-well plate at a density of 35×10^3 cells/well in their complete cell culture medium (MEM with 10% FBS). After 24 h, the medium was changed for MEM containing D-glucose (Sigma Aldrich) at the final concentrations of 25 and 50 mM ± 200 ng/mL of mNGF, and cells were incubated for 2 days. At *day 3*, the medium was replaced with fresh medium with a new portion of D-glucose ± mNGF without FBS, and the scratch test was performed as described above. The control group without extra addition of glucose had a final D-glucose concentration of 5.5 mM.

Keratinocytes were seeded in a 24-well plate at a density of 5.0×10^4 cells/well in their complete culture medium without FBS. At 7 days in vitro (DIV), the keratinocytes reached a density of 90%. The medium was changed, D-glucose (Sigma Aldrich) was added at the final concentrations of 5.5, 10, and 25 mM ± 200 ng/mL mNGF, and the cells were incubated overnight. The medium was replaced with a new portion of D-glucose ± NGF without FBS, and the scratch test was performed as described above. The control group is represented by the glucose vehicle (PBS). The culture was maintained for 48 h.

Glucose treatment and tube formation assay. HUVECs were seeded in a 24-well plate with a density of 9×10^4 cells/well on gelatin coating in culture medium containing mNGF (200 ng/mL) and D-glucose (30 mM) overnight in a humidified incubator of 5% CO_2 at 37°C. The next day, the cells were detached using Trypsin EDTA and seeded on Geltrex LDEV-free matrix in the culture medium with mNGF (200 ng/mL) and D-glucose (30 mM) for tube formation assay. The control group was represented by the glucose vehicle (PBS). The assay was blocked after 8 h, this being the time of maximum tube net extension under the experimental conditions used.

RNA isolation and reverse transcription. Total RNA isolation was performed using the RNeasy Micro kit (Qiagen, Milan, Italy) following the manufacturer's instructions. Total RNA was eluted in RNase-free water, and the concentration was estimated through absorbance values at 260, 280, and 320 nm (Nanodrop 2000 spectrophotometer; Thermo Scientific). First-strand cDNAs were obtained using the iScript cDNA Synthesis Kit (Bio-Rad), incubating samples at 42°C for 30 min. An RNA sample with no reverse transcriptase enzyme in the reaction mix was processed as a no-reverse transcription control sample.

Semiquantitative real-time PCR and gel electrophoresis. Semiquantitative real-time PCR was performed using the CFX96 real-time PCR system (Bio-Rad). The reactions were performed in a final volume of 20 μL consisting of 1× SYBR Green qPCR master mix (Bio-Rad) and 2 μM forward and reverse primers. To avoid possible contamination of genomic DNA in isolated RNA, the no-reverse transcriptase sample was processed in parallel with the others and tested by real-time PCR for every pair of primers used. All primers used were designed using Primer Blast software (NCBI) and synthesized by Integrated DNA Technologies (Coralville, IA). The following primer sequences were used: TrkA, forward: 5′-CCCCATCCCTGACACTAACA-3′ and reverse: 5′-GCACAAGGAGCAGCGTAGAA-3′; p75, forward: 5′-ACCAGGGATGGTACTAGGGG-3′and reverse: 5′-GTCCATGGCTCTGGTTCCTC-3′; GAPDH, forward: 5′-TCATCCCTGCCTCTACTG-3′ and reverse: 5′-TGCTTCACCACCTTCTTG-3′ was used as a housekeeping gene for an internal control. The thermal profile of the PCR reactions initially consisted of a denaturation step (98°C, 3 min) and 40 cycles of amplification (95°C for 10 s and 60°C for 60 s). At the end of the amplification cycles, the melting curve of the amplified products was performed according to the following temperature/time scheme: heating from 55 to 95°C with a temperature increase of 0.5°C/s. Primer efficiency values for all primers were 95–102%. Because of the high cycle quantification values, the PCR products were detected by electrophoresis on 2% agarose gel (Sigma Aldrich) and visualized with GelRed (Biotium) staining under ultraviolet (UV) light (Bio-Rad). The correct PCR products following amplification should have the following dimensions: 175 base pairs (bp) for GAPDH, 131 bp for TrkA, and 77 bp for p75. As a reference for the bands obtained on the gel, the 100-bp Plus DNA Ladder (Thermo Fisher) was used.

Statistical analysis. Results were derived from triplicate cell experiments, expressed as means ± SE, and plotted on graphs. Statistical analyses were performed with Prism software (GraphPad), using the Student's *t* test to compare the two groups; one-way ANOVA followed by Tukey's multiple-comparisons test for dose-response experiments; and two-way ANOVA followed by Dunnett's multiple-comparisons test for time- and treatment-response experiments (see RESULTS and key to Figs. 1–6 for details). Results were considered significant when the probability of their occurrence as a result of chance alone was <5% ($P < 0.05$).

RESULTS

TrkA and p75 expression in BJ cells, HEKa cells, and HUVECs. The three cell lines were first characterized to evaluate the expression of specific markers, i.e., keratin and laminin for keratinocytes, vimentin for fibroblasts, and VE-cadherin and PECAM1 for HUVECs. The immunocytochemical staining results are presented in Fig. 1, where Fig. 1*A* shows laminin (red, *Aa*) and keratin (green, *Ab*) double staining in the cytoplasm of keratinocytes; Fig. 1*F* shows the fibrillary distribution of vimentin in the cytoplasm of fibroblasts; Fig. 1*K* shows VE-cadherin (red, *Ka*) and PECAM1 (green, *Kb*) double staining in HUVEC, which decorate the plasma membrane.

The presence of TrkA and p75 receptors was assessed by immunocytochemistry in the basal condition and after mNGF stimulation (100 ng/mL). Whereas the basal expression of both TrkA and p75 proteins is quite low in all cell types [TrkA: keratinocytes (Fig. 1*B*), fibroblasts (Fig. 1*G*) and HUVEC (Fig. 1*L*); p75: keratinocytes (Fig. 1*D*), fibroblasts (Fig. 1*I*), and HUVEC (Fig. 1*N*)], exposure to NGF strongly increases TrkA immunostaining in keratinocytes (Fig. 1*C*) and HUVECs (Fig. 1*M*), but not in fibroblasts (Fig. 1*H*), whereas p75 immunostaining increases in keratinocytes (Fig. 1*E*), fibroblasts (Fig. 1*J*), and in endothelial cells (Fig. 1*O*).

We also investigated the expression of TrkA and p75 in basal conditions by real-time PCR and electrophoresis in agarose gel (Fig. 1*P*). The mRNA of both receptors was detected in all three cell types at their basal level, as confirmed by the specific PCR products with the band size 131 bp for TrkA and 77 bp for the p75 receptor.

Effect of mNGF on HEKa cell, BJ cell, and HUVEC proliferation. To evaluate the effect of mNGF on the proliferation of keratinocytes, fibroblasts, and HUVECs, cell cultures were treated for 8 days with mNGF at three different concentrations (50, 100, and 200 ng/mL; Fig. 2*A*). By preliminary experiments, we confirmed that mNGF is more powerful in these cell types compared with rhNGF (Alomone). The results in HEKa are reported in Fig. 2*B*, where representative micrographs of the cell system at 0 and 8 DIV of mNGF exposure are also shown. mNGF induces a dose-dependent increase in cell proliferation [2-way ANOVA, treatment effect $F(3,100) = 83.30$, $P < 0.0001$, time effect $F(4, 00) = 995.5$, $P < 0.0001$], and the results of the post hoc Dunnett's multiple-comparison test are reported. The results in BJ are reported in Fig. 2*C*, where representative micrographs of the cell system at 0 and 8 DIV of mNGF exposure are also shown. mNGF induces an increase in cell proliferation at the highest dose only [2-way ANOVA, treatment effect

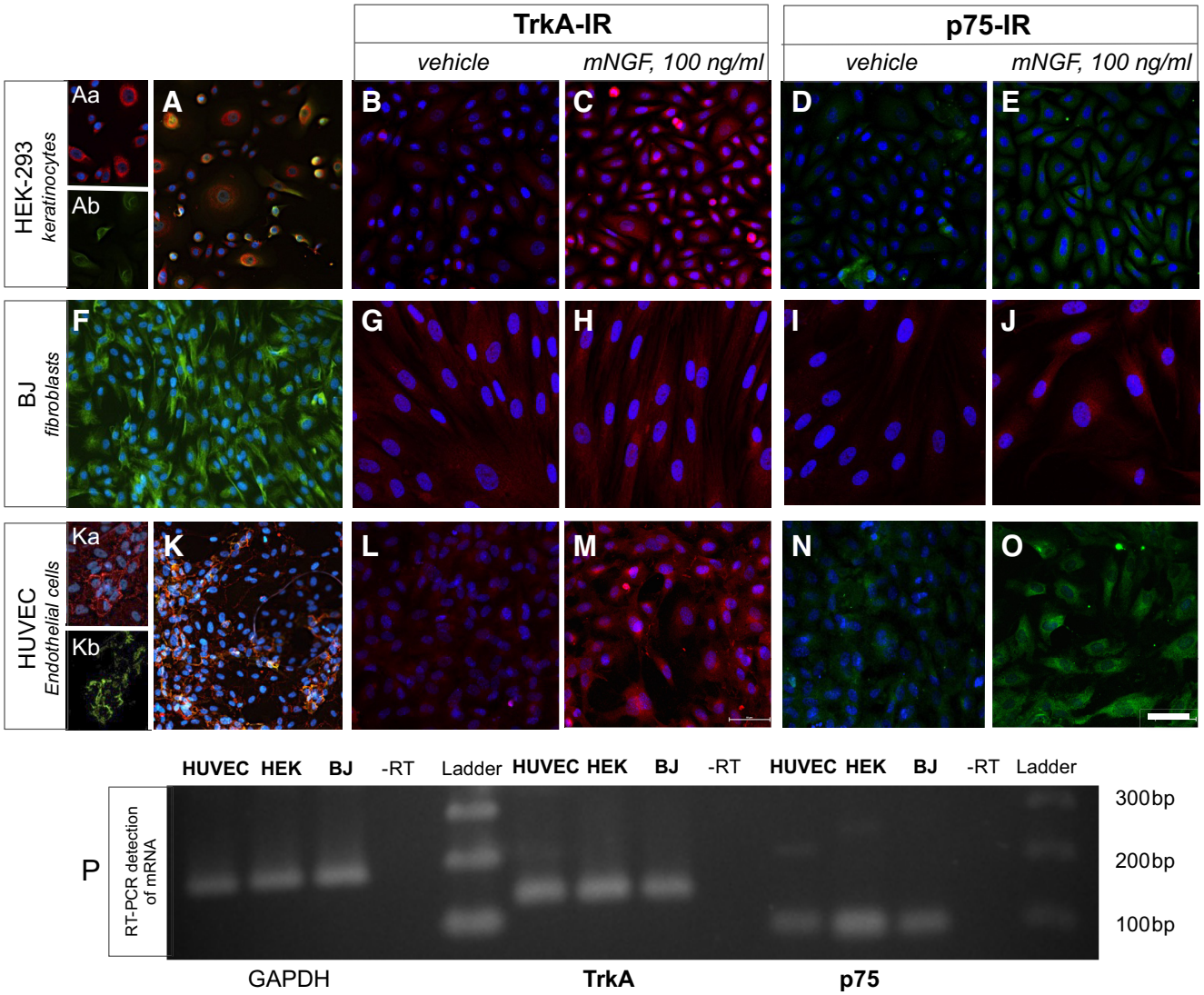

Fig. 1. Normal adult human primary epidermal keratinocyte cell (HEKa, *A–E*), human skin fibroblast cell (BJ, *F–J*), and human umbilical vein endothelial cell (HUVEC, *K–O*) characterization. *A*: laminin (red, *Aa*) and keratin (green, *Ab*) double staining; *F*: vimentin; *K*: VE-cadherin (red, *Ka*) and platelet/endothelial cell adhesion molecule-1 (PECAM1, green, *Kb*) double staining. The expression of tropomyosin receptor kinase A (TrkA) and p75 in basal conditions is shown in *B* and *D* (HEKa), *G* and *I* (BJ), and *L* and *N* (HUVEC), whereas after nerve growth factor (NGF) exposure is shown in *C* and *E* (HEKa), *H* and *J* (BJ), and *M* and *O* (HUVEC), respectively. IR, immunoreactive. *P*: PCR products with band size 131 bp for TrkA and 77 bp for neurotrophin low-affinity receptor (p75). mNGF, mouse NGF. Bar = 50 μm.

$F(3,39) = 3.667$, $P = 0.0202$, time effect $F(4,39) = 47.29$, $P < 0.0001$], and the results of the post hoc Dunnett's multiple-comparison test are reported. The results in HUVEC are reported in Fig. 2*C*, where representative micrographs of the cell system at 0 and 8 DIV of NGF exposure are also shown. mNGF induces a dose-dependent increase in cell proliferation [2-way ANOVA, treatment effect $F(12,32) = 6.008$, $P = 0.0202$, time effect $F(4,32) = 632,4$, $P < 0.0001$], and the results of the post hoc Dunnett's multiple-comparison test are reported. To further explore the NGF effect on HUVEC, we evaluated the tube formation assay by treating cells seeded on Geltrex overnight with mNGF at three different concentrations (50, 100, and 200 ng/mL). The results are reported in Fig. 2*D*, where representative micrographs of the cell system at 0 and 8 h of mNGF exposure are also shown. mNGF induces a dose-dependent increase in the number of segments [2-way ANOVA, treatment effect $F(3,96) = 60.15$, $P < 0.0001$, time effect $F(2,96) = 254.9$, $P < 0.0001$], and the results of the post hoc Dunnett's multiple-comparison test are reported. Similar effects are also observed in the other parameters of the angiogenesis assay (mashes, no. of junctions, no. of nodes, no. of branches; data not shown).

In the same experimental conditions, we also evaluated the effect of NGF exposure on the expression of the cell cycle-associated marker MCM2. The immunocytochemical staining is presented in Fig. 3, where results for Hoechst (blue, *A–F*) and MCM2 positivity (red, *G–L*) in all cell lines are shown. The effect of NGF on proliferation was expressed as a percentage of MCM2-IR versus Hoechst-positive cells, and results are reported in Fig. 3, *Q* (keratinocytes), *R* (fibroblast), and *S* (HUVEC), respectively. NGF exposure increases the number of MCM2-positive cells in keratinocytes (unpaired *t* test, $P =$

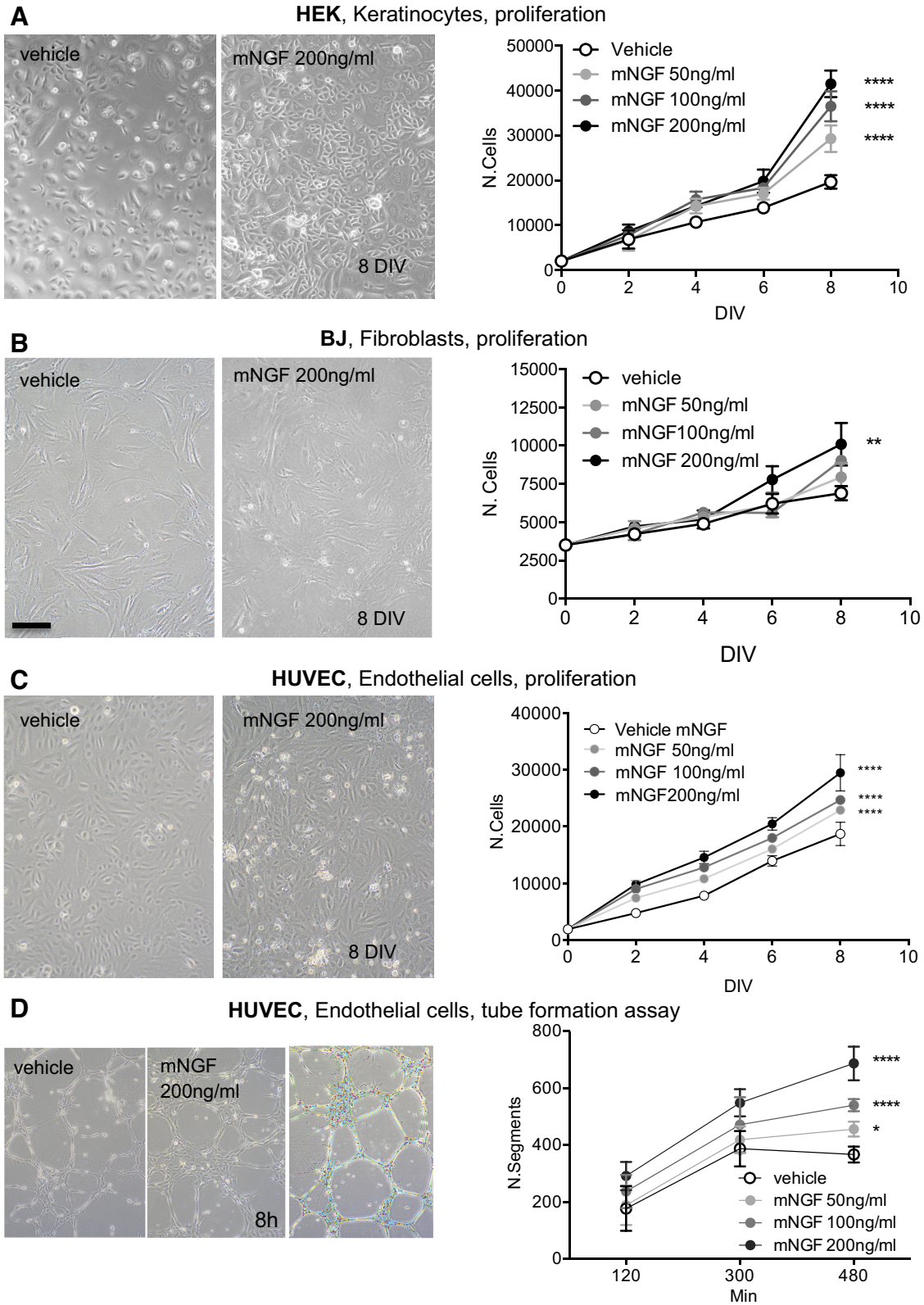

Fig. 2. Dose-response effect of nerve growth factor (NGF) treatment on normal adult human primary epidermal keratinocyte cell (HEKa, *A*), human skin fibroblast cell (BJ, *B*), and human umbilical vein endothelial cell (HUVEC, *C*) proliferation and tube formation assay (*D*). Representative micrographs of the cell systems are reported in *A*–*C*. DIV, days in vitro. Data are derived from independent triplicate experiments and are expressed as means + SE. Statistical analysis: 2-way ANOVA and post hoc test, $*P < 0.05$, $**P < 0.01$, and $****P < 0.0001$.

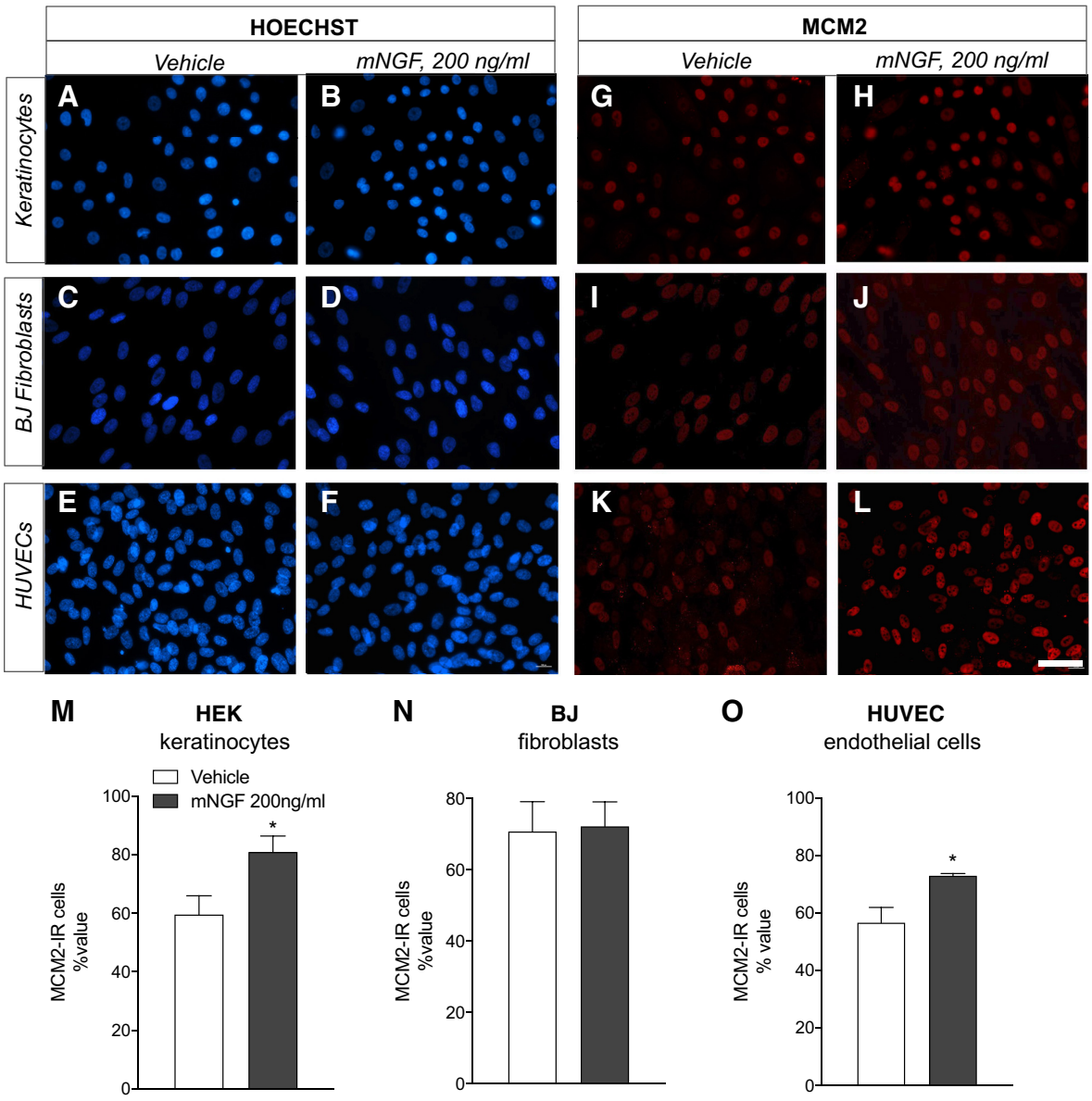

Fig. 3. Hoechst staining (*A–F*) and minichromosome maintenance complex component 2 (MCM2-IR, *G–L*) in normal adult human primary epidermal keratinocyte cells (HEKa cells), human skin fibroblast cells (BJ cells), and human umbilical vein endothelial cells (HUVEC) exposed to 200 ng/mL mouse nerve growth factor (mNGF) and vehicle. The percentage of MCM2-positive cells is presented in *Q–S*. IR, immunoreactive. Data are derived from independent triplicate experiments and are expressed as means + SE. Statistical analysis: *t* test, $^*P < 0.05$. Bar = 50 μm.

0.0128) and HUVEC (unpaired *t* test, $P = 0.0311$) but is ineffective in fibroblasts.

Effect of mNGF on wound healing assay. To evaluate the effect of mNGF on cell migration, keratinocytes and fibroblasts were tested in the in vitro wound healing assay, after treatment with increasing concentrations of this factor (50, 100, and 200 ng/mL) overnight at 7 DIV for keratinocytes (Fig. 4*A*) and at 2 DIV for fibroblasts (Fig. 4*B*). The test was performed the day after this treatment, measuring the percent of closure 8–10 h after the scratch was made [HEK (Fig. 5*C*) and BJ (Fig. 4*D*) cells]. As a control, a mNGF neutralization experiment was carried out on both cell lines, using the culture medium enriched with 200 ng/mL mNGF preincubated overnight with 10 μg/mL anti-mNGF antibody. The results are presented in Fig. 4, *C* (keratinocytes) and *D* (fibroblasts), where representative micrographs of the control and mNGF-treated cultures are also shown. The statistical analysis was performed by one-way ANOVA for the mNGF effect, with the vehicle-treated culture as the control group (Dunnett's post hoc test, $P < 0.05$ and $P < 0.0001$), and by Student's *t* test for the anti-NGF Ab group, compared with 200 mg/mL NGF ($P < 0.05$ and $P < 0.0001$). mNGF promotes wound closure by HEKa cells in a dose-dependent manner, and this effect abolishes NGF neutralization. In contrast, a very small nonsignificant effect on BJ wound closure is observed, although NGF neutralization reduces wound closure.

Effect of mNGF on wound healing and tube formation assay performed in hyperglycemic medium. Because diabetes is a pathological condition that significantly impairs the wound healing process, we wanted to evaluate the effect of in vitro

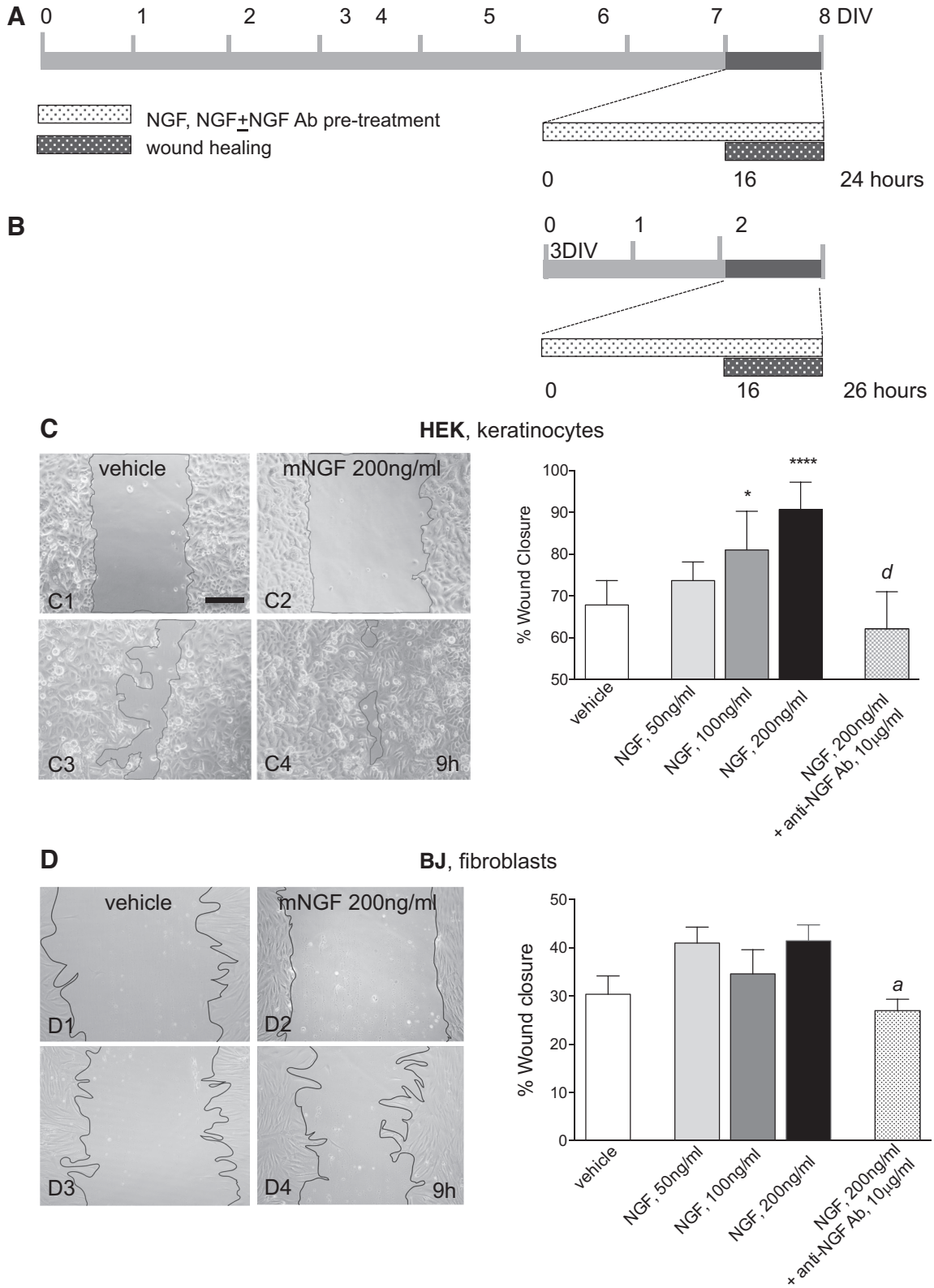

Fig. 4. Effect of 200 ng/mL nerve growth factor (NGF) and anti-NGF Ab exposure on wound assay performed using normal adult human primary epidermal keratinocyte (HEKa, *C*) and human skin fibroblast (BJ, *D*) cells. The experimental schema used for HEK and BJ cells is presented in *A* and *B*, respectively. Micrographs show representative images of vehicle- and mouse nerve growth factor (mNGF)-exposed cells at scratch and 9 h after scratch. DIV, days in vitro. Results derive from independent triplicate experiments and are expressed as means + SE. Statistical analysis: NGF effect, 1-way ANOVA and post hoc test, $^{*}P < 0.05$ and $^{****}P < 0.0001$; anti-NGF Ab, Student's *t* test, $^{a}P < 0.01$ and $^{d}P < 0.0001$.

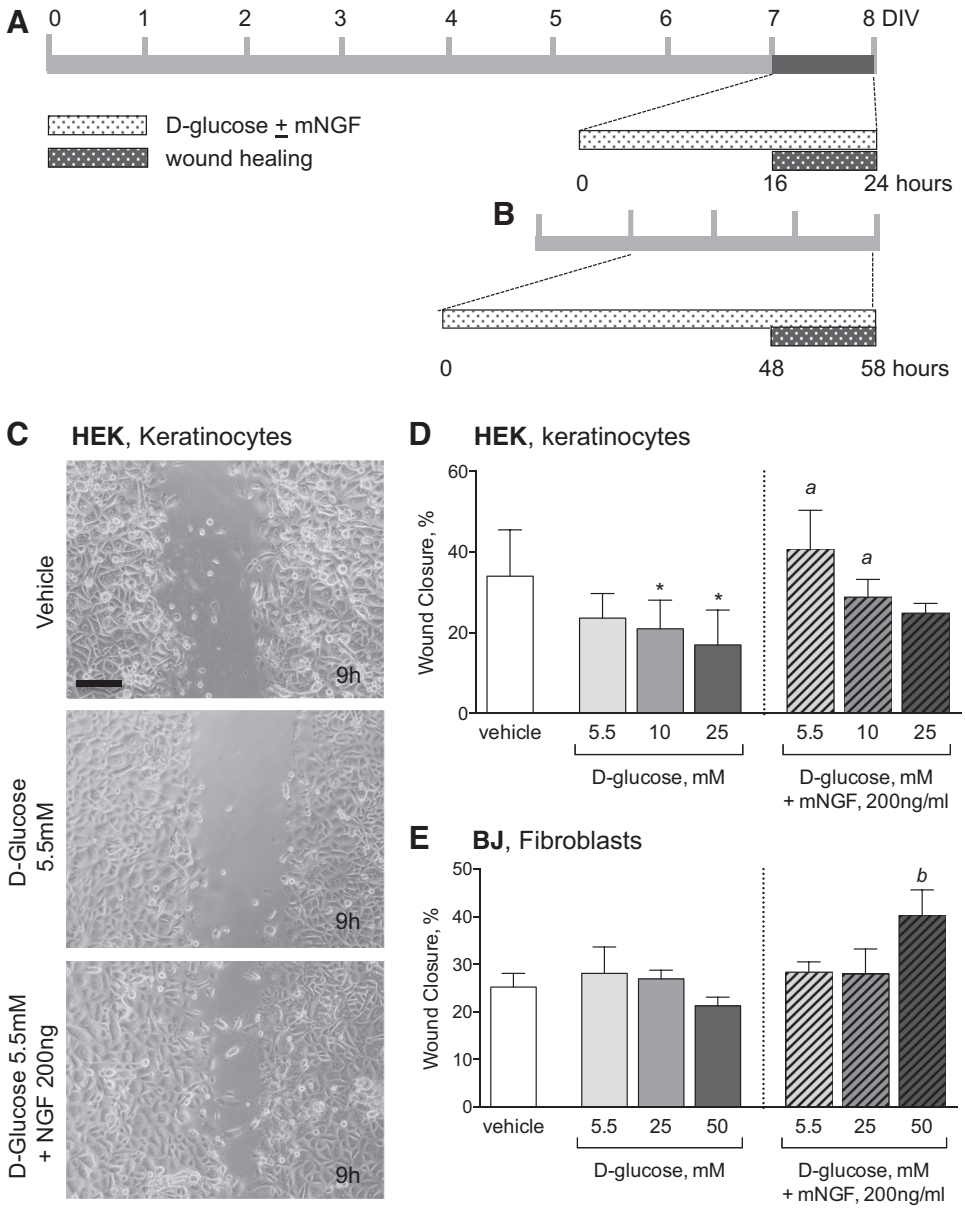

Fig. 5. Effect of nerve growth factor (NGF) treatment on wound in a hyperglycemic culture media. The experimental schema used for normal human primary epidermal keratinocyte (HEK) and human skin fibroblast (BJ) cells is presented in *A* and *B*, respectively. Micrographs show representative images of vehicle and mouse nerve growth factor (mNGF)-exposed HEK cells at 9 h after scratch in the different experimental conditions (*C*), and results are reported in *D* (HEK) and *E* (BJ). IR, immunoreactive; DIV, days in vitro. Results derive from independent triplicate experiments and are expressed as means + SE. Statistical analysis: 1-way ANOVA and post hoc test, $^{*}P < 0.05$; anti-NGF Ab, Student's *t* test, $^{a}P < 0.01$ and $^{b}P < 0.05$.

hyperglycemia on cell keratinocyte and fibroblast migration (Fig. 5) and on tube formation by endothelial cells (angiogenesis assay; Fig. 6). We first performed the in vitro wound assay by culturing HEKa and BJ cells in the presence of increasing D-glucose concentrations for 24 h (HEKa) and for 2 days (BJ). The experimental schedule is shown in Fig. 5, *A* (HEKa) and *B* (BJ), and the results are reported in Fig. 5, *D* (HEKa) and *E* (BJ), where representative micrographs of HEK cells in different experimental conditions are shown (Fig. 5*C*). The statistical analysis was performed by one-way ANOVA for the mNGF effect, with the vehicle-treated culture as the control group (Dunnett's post hoc test, $P < 0.05$). We observed a dose-dependent decrease of the percent of wound closure in HEKa cells while hyperglycemia does not affect wound closure in BJ cells. In addition, the angiogenesis performed with HUVECs is significantly modified by culturing cells in hyperglycemia during both the gelatin and Geltrex seeding, as indicated by the strong decrease in the number of master junctions and segments ($P < 0.0001$; Fig. 5). We then explored the mNGF effect on this impairment by adding 200 ng/mL mNGF to the hyperglycemia medium. We observed that mNGF reverts the migration impairment observed in HEKa keratinocytes (Student's *t* test for the respective D-glucose concentration, $P < 0.05$; Fig. 5*D*). In BJ fibroblasts, an increase in wound closure was observed at the highest D-glucose concentration (Student's *t* test for the respective D-glucose concentration, $P < 0.01$; Fig. 5*E*).

The results of the HUVEC angiogenesis assay are shown in Fig. 6, *E* and *G*, where the time-dependent increase of two main parameters of the analysis, i.e., the number of master junctions and of the master segments, is presented. mNGF completely reverts the impairment in the angiogenesis assay produced by culturing HUVECs in a hyperglycemic medium [2-way ANOVA, master junction: treatment effect $F(3,101) = 169.5$, $P < 0.0001$, time effect $F(2,101) = 127.1$, $P < 0.0001$; master segments: $F(3,108) = 175.2$, $P < 0.0001$, time effect $F(2,108) = 264.9$, $P < 0.0001$].

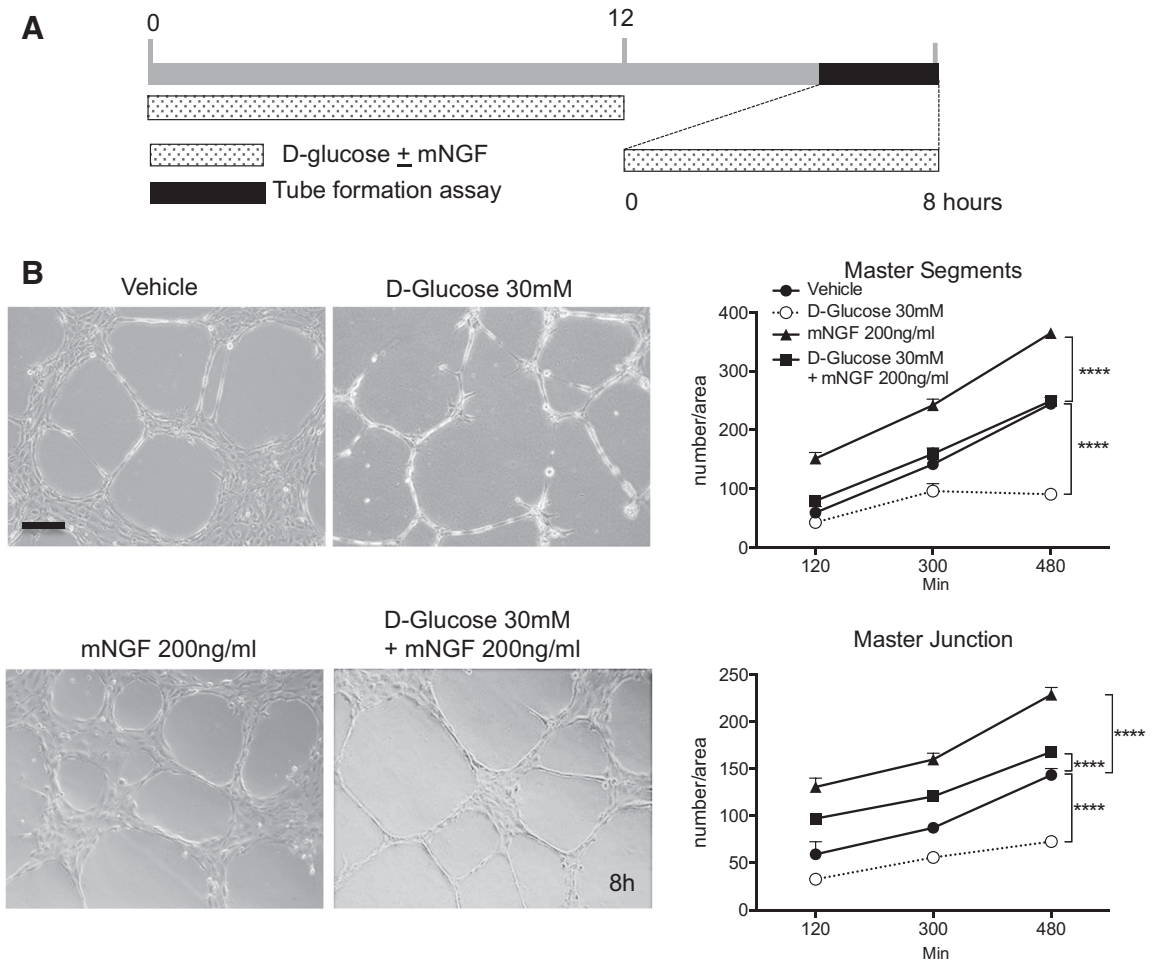

Fig. 6. Effect of nerve growth factor (NGF) treatment on tube formation assay in a hyperglycemia culture medium. The experimental schema is presented in *A*. Micrographs show representative images of vehicle and mouse nerve growth factor (mNGF) exposed in the different experimental conditions, and results relative to major angiogenic assay parameters are reported. DIV, days in vitro. Results derive from independent triplicate experiments and are expressed as means + SE. Statistical analysis: one-way ANOVA, $****P < 0.0001$.

DISCUSSION

Wound healing in epithelial tissues is a complex process that involves many resident and migrating cells in a well-orchestrated temporal sequence. An impairment in this process may lead to chronic lesions, such as chronic skin or corneal ulcers, compromising tissue and organ function and leading to severe chronic disabilities. Wound healing is largely dependent on endogenous regenerative capability, with respect to which the large family of growth and trophic factors plays a major role. Over the last few years, a role of NGF in epithelial wound healing has emerged (8), and the first rhNGF drug has been approved by the FDA for rare neurotrophic keratitis. However, the cellular and molecular targets of the NGF prohealing effects are not completely understood. In this study, we then explored, in in vitro simplified systems, the effect of mNGF on the main cellular processes, i.e., cell proliferation and migration, of keratinocytes, fibroblasts, and endothelial cells (see Table 1 for a summary of the results). Keratinocytes are responsible for re-epithelization, fibroblasts for extracellular matrix deposition, and endothelial cells for neoangiogenesis (45), in a continuous cellular and molecular cross talk that finally leads to epithelial tissue repair.

The first cell type we investigated were keratinocytes, using the HEKa cell line, one of the most widely used cell lines, both

Table 1. *Summary of the mNGF effects on the cell lines included in this study*

	Control Medium			Hyperglycemic Medium	
	Proliferation	Migration (Scratch assay)	Angiogenesis (Tube formation assay)	Migration (Scratch assay)	Angiogenesis (Tube formation assay)
HEK	↑	↑		↑	
BJ	↑ =	=		↑ =	
HUVEC	↑		↑		↑

mNGF, mouse nerve growth factor; HEK, normal human primary epidermal keratinocyte cells; BJ, human skin fibroblast cells; HUVEC, human umbilical vein endothelial cells; ↑, increase; =, no changes.

in research and for drug approval (10). HEKa cells express TrkA high-affinity and p75 low-affinity receptors, as already described in isolated primary keratinocytes, where they increase during the exponential growth phase (9), as well as in the basal layer of the epidermis, where proliferating cells reside (40), an effect mediated by TrkA. In fact, inhibition of TrkA phosphorylation reduces the proliferation of keratinocytes in culture (40), and TrkA inhibition reduces the expression of pAkt/Akt and pERK/ERK1/2, thus reducing cellular proliferation (58). Moreover, TrkA and p75 are widely expressed in cells in the soft tissues of the human oral cavity, including keratinocytes, endothelial cells, fibroblasts, and leukocytes, and in ductal and acinar cells of all types of salivary glands (46).

We observed that HEKa cells strongly respond, in a dose-responsive manner, to NGF exposure by increasing proliferation and migration in the wound assay. Normal human keratinocytes synthesize and release high amounts of biologically active NGF, considered a key player of an autocrine loop, acting as a mitogen and survival factor for human keratinocytes, as indicated by the protection against UV-induced apoptosis (27). NGF released from keratinocytes also exerts paracrine functions on human melanocytes by stimulating their dendricity and protecting them from cell death (55). NGF is also a crucial neurotrophic molecule for skin innervation (16, 33), and the overall aforementioned findings strongly suggest that NGF should be regarded as an important growth factor in both intact and diseased epidermis (48).

The second type of cells included in this study is dermal fibroblasts, through the BJ cell line, also widely used for drug screening (11). Dermal fibroblasts play a crucial role in the wound healing process, being attracted from the edge of the wound, releasing various chemokines at the inflammation stage, and secreting a large number of extracellular matrix proteins, mainly collagen. Results from our study indicate that BJ dermal fibroblasts, although they express high-affinity NGF receptors, are poorly regulated by exogenous NGF administration in terms of proliferation and migration in the absence of other stimuli. Interestingly, several reports suggest that, in inflammatory/immune conditions, such as allergic inflammation (31) or articular inflammation (37, 52), fibroblasts are one of the sources and targets of NGF via the TrkA receptor.

Finally, we investigated the effect of NGF on HUVECs, the pivot cell for in vitro angiogenesis assays, confirming the expression of both TrkA and p75 already demonstrated by RT-PCR analysis, Western blotting (6), and immunocytochemistry (41). We observed a substantial proangiogenic effect of mNGF in the 3D environment, thus confirming the stimulating effect of NGF on the proliferation of HUVEC, also described in human choroidal endothelial cells (50) and human dermal microvascular endothelial cells (42). Consistent in vivo evidence also supports an angiogenic effect of NGF in different tissues and conditions, such as in deafferented peripheral sympathetic ganglia (5), the chorioallantoic membrane of the chicken embryo (50), gastric mucosal injury (1), ischemic brain (19), and rat retina (54).

Wound healing is impaired in various pathological conditions, and diabetes is probably the most widespread medical condition leading to chronic pathologies characterized by defective endogenous regeneration, chronic skin ulcers in the condition known as "diabetic foot," representing a severe and still unmet medical need (17). Several lines of evidence converge in indicating NGF as a major player in the wound healing process in diabetes (53). In vivo studies indicate that an NGF defect compromises tendon healing (2); different treatments that increase endogenous NGF availability promote wound healing (35, 39, 44), whereas topical NGF application in different skin wound models in diabetic rodents promotes and accelerates healing (13, 28, 34), as observed in humans also (12).

We then explored the effect of NGF on the proliferation and migration of keratinocytes, fibroblasts, and endothelial cells in hyperglycemia (20, 25). The migration and tube formation of keratinocytes and HUVECs significantly decrease in high-D-glucose concentration while fibroblasts are unaffected. The effects of a high-glucose environment on the physiological function of keratinocytes, including impaired proliferation and migration, are well known (15), and in vitro studies also describe the effects of high glucose concentration on the growth and survival of various types of endothelial cells, including HUVECs (30, 56). We demonstrated that the hyperglycemia-induced defects are completely reverted by the concomitant presence of NGF in the culture medium, which restores and even improves the proliferative capability of HEKa cells and tube formation by HUVECs compared with normoglycemia.

Our experiments do not currently include molecular end points useful for exploring the molecular mechanism by which NGF exerts the observed effects, either directly or interacting with other growth factors and hormones present in the culture medium, in particular in reversing high-glucose impairment of proliferation and tube formation. However, several hypotheses can be suggested. For example, NGF and its high-affinity receptor TrkA promote cell survival and proliferation by activating the signaling pathways of extracellular signal-regulated kinase (ERK), phosphatidylinositide 3-kinase (PI3K)/AKT1, and p38 mitogen-activated protein kinase (26, 41) in a time-dependent and dose-dependent manner (14). The ERK signaling pathway activates HUVEC proliferation (49), whereas the inhibition of endothelial cell proliferation by a high glucose concentration also involves ERK1/2 pathways (7). Moreover, recent studies show that NGF functions as an indirect activator of angiogenesis by inducing specific molecules, such as vascular endothelial growth factor (VEGF; see Refs. 5, 23, 47, and 57).

In conclusion, by using HEKa cells, BJ cells, and HUVECs, we identified keratinocytes and endothelial cells as NGF-sensitive cells, whereas fibroblasts do not directly respond to NGF stimulation. Moreover, we also demonstrated that NGF is able to repair the defects of keratinocyte proliferation and endothelial cell tube formation induced by a high-glucose microenvironment. These results strongly support the view of NGF as a pleiotropic molecule, also providing a further rationale for the therapeutic use of NGF in epithelial tissue wound care.

ACKNOWLEDGMENTS

Present address of Natalia Gostynska: Neuroscience and Brain Technology, Istituto Italiano di Tecnologia, Via Morego 30, 16163 Genova, Italy.

GRANTS

This study was supported by the IRMI project (Italian Regenerative Medicine Infrastructure), the Italian Ministry of Education, University and Research (CTN01_00177_888744).

DISCLOSURES

No conflicts of interest, financial or otherwise, are declared by the authors.

AUTHOR CONTRIBUTIONS

L.C. conceived and designed research; N.G., M.P., M.L.R., and L.A. performed experiments; N.G., M.P., and L.C. analyzed data; L.G. and L.C. interpreted results of experiments; N.G. and M.P. prepared figures; N.G., M.P., and L.C. drafted manuscript; N.G., M.P., M.L.R., L.G., L.A., and L.C. approved final version of manuscript; L.G. and L.A. edited and revised manuscript.

REFERENCES

1. **Ahluwalia A, Jones MK, Brzozowski T, Tarnawski AS.** Nerve growth factor is critical requirement for in vitro angiogenesis in gastric endothelial cells. *Am J Physiol Gastrointest Liver Physiol* 311: G981–G987, 2016. doi:10.1152/ajpgi.00334.2016.
2. **Ahmed AS, Li J, Abdul AM, Ahmed M, Östenson CG, Salo PT, Hewitt C, Hart DA, Ackermann PW.** Compromised neurotrophic and angiogenic regenerative capability during tendon healing in a rat model of type-II diabetes. *PLoS One* 12: e0170748, 2017. doi:10.1371/journal.pone.0170748.
3. **Aloe L, Calzà L.** *NGF and related molecules in health and disease*. In: *Progress in Brain Research*. Amsterdam, The Netherlands: Elsevier, 2003, vol. 146.
4. **Bocchini V, Angeletti PU.** The nerve growth factor: purification as a 30,000-molecular-weight protein. *Proc Natl Acad Sci USA* 64: 787–794, 1969. doi:10.1073/pnas.64.2.787.
5. **Calza L, Giardino L, Giuliani A, Aloe L, Levi-Montalcini R.** Nerve growth factor control of neuronal expression of angiogenetic and vasoactive factors. *Proc Natl Acad Sci USA* 98: 4160–4165, 2001. doi:10.1073/pnas.051626998.
6. **Cantarella G, Lempereur L, Presta M, Ribatti D, Lombardo G, Lazarovici P, Zappalà G, Pafumi C, Bernardini R.** Nerve growth factor-endothelial cell interaction leads to angiogenesis in vitro and in vivo. *FASEB J* 16: 1307–1309, 2002. doi:10.1096/fj.01-1000fje.
7. **Chen YH, Guh JY, Chuang TD, Chen HC, Chiou SJ, Huang JS, Yang YL, Chuang LY.** High glucose decreases endothelial cell proliferation via the extracellular signal regulated kinase/p15(INK4b) pathway. *Arch Biochem Biophys* 465: 164–171, 2007. doi:10.1016/j.abb.2007.05.010.
8. **Chéret J, Lebonvallet N, Carré JL, Misery L, Le Gall-Ianotto C.** Role of neuropeptides, neurotrophins, and neurohormones in skin wound healing. *Wound Repair Regen* 21: 772–788, 2013. doi:10.1111/wrr.12101.
9. **Di Marco E, Mathor M, Bondanza S, Cutuli N, Marchisio PC, Cancedda R, De Luca M.** Nerve growth factor binds to normal human keratinocytes through high and low affinity receptors and stimulates their growth by a novel autocrine loop. *J Biol Chem* 268: 22838–22846, 1993.
10. **Dumont J, Euwart D, Mei B, Estes S, Kshirsagar R.** Human cell lines for biopharmaceutical manufacturing: history, status, and future perspectives. *Crit Rev Biotechnol* 36: 1110–1122, 2016. doi:10.3109/07388551.2015.1084266.
11. **Eignerova B, Tichy M, Krasulova J, Kvasnica M, Rarova L, Christova R, Urban M, Bednarczyk-Cwynar B, Hajduch M, Sarek J.** Synthesis and antiproliferative properties of new hydrophilic esters of triterpenic acids. *Eur J Med Chem* 140: 403–420, 2017. doi:10.1016/j.ejmech.2017.09.041.
12. **Generini S, Tuveri MA, Matucci Cerinic M, Mastinu F, Manni L, Aloe L.** Topical application of nerve growth factor in human diabetic foot ulcers. A study of three cases. *Exp Clin Endocrinol Diabetes* 112: 542–544, 2004. doi:10.1055/s-2004-821313.
13. **Graiani G, Emanueli C, Desortes E, Van Linthout S, Pinna A, Figueroa CD, Manni L, Madeddu P.** Nerve growth factor promotes reparative angiogenesis and inhibits endothelial apoptosis in cutaneous wounds of Type 1 diabetic mice. *Diabetologia* 47: 1047–1054, 2004. doi:10.1007/s00125-004-1414-7.
14. **Hong J, Qian T, Le Q, Sun X, Wu J, Chen J, Yu X, Xu J.** NGF promotes cell cycle progression by regulating D-type cyclins via PI3K/Akt and MAPK/Erk activation in human corneal epithelial cells. *Mol Vis* 18: 758–764, 2012.
15. **Hu SC, Lan CE.** High-glucose environment disturbs the physiologic functions of keratinocytes: Focusing on diabetic wound healing. *J Dermatol Sci* 84: 121–127, 2016. doi:10.1016/j.jdermsci.2016.07.008.
16. **Indo Y.** Nerve growth factor, pain, itch and inflammation: lessons from congenital insensitivity to pain with anhidrosis. *Expert Rev Neurother* 10: 1707–1724, 2010. doi:10.1586/ern.10.154.
17. **Jeffcoate WJ, Vileikyte L, Boyko EJ, Armstrong DG, Boulton AJM.** Current challenges and opportunities in the prevention and management of diabetic foot ulcers. *Diabetes Care* 41: 645–652, 2018. doi:10.2337/dc17-1836.
18. **Kawamoto K, Matsuda H.** Nerve growth factor and wound healing. *Prog Brain Res* 146: 369–384, 2004. doi:10.1016/S0079-6123(03)46023-8.
19. **Kim YS, Jo DH, Lee H, Kim JH, Kim KW, Kim JH.** Nerve growth factor-mediated vascular endothelial growth factor expression of astrocyte in retinal vascular development. *Biochem Biophys Res Commun* 431: 740–745, 2013. doi:10.1016/j.bbrc.2013.01.045.
20. **Kruse CR, Singh M, Sørensen JA, Eriksson E, Nuutila K.** The effect of local hyperglycemia on skin cells in vitro and on wound healing in euglycemic rats. *J Surg Res* 206: 418–426, 2016. doi:10.1016/j.jss.2016.08.060.
21. **Lambiase A, Manni L, Bonini S, Rama P, Micera A, Aloe L.** Nerve growth factor promotes corneal healing: structural, biochemical, and molecular analyses of rat and human corneas. *Invest Ophthalmol Vis Sci* 41: 1063–1069, 2000.
22. **Lambiase A, Rama P, Bonini S, Caprioglio G, Aloe L.** Topical treatment with nerve growth factor for corneal neurotrophic ulcers. *N Engl J Med* 338: 1174–1180, 1998. doi:10.1056/NEJM199804233381702.
23. **Lamers ML, Almeida ME, Vicente-Manzanares M, Horwitz AF, Santos MF.** High glucose-mediated oxidative stress impairs cell migration. *PLoS One* 6: e22865, 2011. doi:10.1371/journal.pone.0022865.
24. **Levi-Montalcini R.** The nerve growth factor 35 years later. *Science* 237: 1154–1162, 1987. doi:10.1126/science.3306916.
25. **Levi-Montalcini R.** *The Saga of the Nerve Growth Factor*. London, UK: World Scientific, 1997.
26. **Li X, Li F, Ling L, Li C, Zhong Y.** Intranasal administration of nerve growth factor promotes angiogenesis via activation of PI3K/Akt signaling following cerebral infarction in rats. *Am J Transl Res* 10: 3481–3492, 2018.
27. **Marconi A, Vaschieri C, Zanoli S, Giannetti A, Pincelli C.** Nerve growth factor protects human keratinocytes from ultraviolet-B-induced apoptosis. *J Invest Dermatol* 113: 920–927, 1999. doi:10.1046/j.1523-1747.1999.00773.x.
28. **Matsuda H, Koyama H, Sato H, Sawada J, Itakura A, Tanaka A, Matsumoto M, Konno K, Ushio H, Matsuda K.** Role of nerve growth factor in cutaneous wound healing: accelerating effects in normal and healing-impaired diabetic mice. *J Exp Med* 187: 297–306, 1998. doi:10.1084/jem.187.3.297.
29. **Matsumura S, Terao M, Murota H, Katayama I.** Th2 cytokines enhance TrkA expression, upregulate proliferation, and downregulate differentiation of keratinocytes. *J Dermatol Sci* 78: 215–223, 2015. doi:10.1016/j.jdermsci.2015.02.021.
30. **McGinn S, Saad S, Poronnik P, Pollock CA.** High glucose-mediated effects on endothelial cell proliferation occur via p38 MAP kinase. *Am J Physiol Endocrinol Metab* 285: E708–E717, 2003. doi:10.1152/ajpendo.00572.2002.
31. **Micera A, Puxeddu I, Aloe L, Levi-Schaffer F.** New insights on the involvement of Nerve Growth Factor in allergic inflammation and fibrosis. *Cytokine Growth Factor Rev* 14: 369–374, 2003. doi:10.1016/S1359-6101(03)00047-9.
32. **Minnone G, De Benedetti F, Bracci-Laudiero L.** NGF and its receptors in the regulation of inflammatory response. *Int J Mol Sci* 18: E1028, 2017. doi:10.3390/ijms18051028.
33. **Montaño JA, Pérez-Piñera P, García-Suárez O, Cobo J, Vega JA.** Development and neuronal dependence of cutaneous sensory nerve formations: Lessons from neurotrophins. *Microsc Res Tech* 73: 513–529, 2010. doi:10.1002/jemt.20790.
34. **Muangman P, Muffley LA, Anthony JP, Spenny ML, Underwood RA, Olerud JE, Gibran NS.** Nerve growth factor accelerates wound healing in diabetic mice. *Wound Repair Regen* 12: 44–52, 2004. doi:10.1111/j.1067-1927.2004.012110.x-1.
35. **Nakagaki O, Miyoshi H, Sawada T, Atsumi T, Kondo T, Atsumi T.** Epalrestat improves diabetic wound healing via increased expression of

nerve growth factor. *Exp Clin Endocrinol Diabetes* 121: 84–89, 2013. doi:10.1055/s-0032-1333279.

36. **Nico B, Mangieri D, Benagiano V, Crivellato E, Ribatti D.** Nerve growth factor as an angiogenic factor. *Microvasc Res* 75: 135–141, 2008. doi:10.1016/j.mvr.2007.07.004.
37. **Ohta M, Chosa N, Kyakumoto S, Yokota S, Okubo N, Nemoto A, Kamo M, Joh S, Satoh K, Ishisaki A.** IL-1β and TNF-α suppress TGF-β-promoted NGF expression in periodontal ligament-derived fibroblasts through inactivation of TGF-β-induced Smad2/3- and p38 MAPK-mediated signals. *Int J Mol Med* 42: 1484–1494, 2018. doi:10.3892/ijmm.2018.3714.
38. **Palazzo E, Marconi A, Truzzi F, Dallaglio K, Petrachi T, Humbert P, Schnebert S, Perrier E, Dumas M, Pincelli C.** Role of neurotrophins on dermal fibroblast survival and differentiation. *J Cell Physiol* 227: 1017–1025, 2012. doi:10.1002/jcp.22811.
39. **Peplow PV, Baxter GD.** Gene expression and release of growth factors during delayed wound healing: a review of studies in diabetic animals and possible combined laser phototherapy and growth factor treatment to enhance healing. *Photomed Laser Surg* 30: 617–636, 2012. doi:10.1089/pho.2012.3312.
40. **Pincelli C, Sevignani C, Manfredini R, Grande A, Fantini F, Bracci-Laudiero L, Aloe L, Ferrari S, Cossarizza A, Giannetti A.** Expression and function of nerve growth factor and nerve growth factor receptor on cultured keratinocytes. *J Invest Dermatol* 103: 13–18, 1994. doi:10.1111/1523-1747.ep12388914.
41. **Rahbek UL, Dissing S, Thomassen C, Hansen AJ, Tritsaris K.** Nerve growth factor activates aorta endothelial cells causing PI3K/Akt- and ERK-dependent migration. *Pflugers Arch* 450: 355–361, 2005. doi:10.1007/s00424-005-1436-0.
42. **Raychaudhuri SK, Raychaudhuri SP, Weltman H, Farber EM.** Effect of nerve growth factor on endothelial cell biology: proliferation and adherence molecule expression on human dermal microvascular endothelial cells. *Arch Dermatol Res* 293: 291–295, 2001. doi:10.1007/s004030100224.
43. **Samarasena JB, Ahluwalia A, Tarnawski AS, Shinoura S, Choi KD, Lee JG, Chang KJ.** Expression of nerve growth factor, its TrkA receptor, and several neuropeptides in porcine esophagus. Implications for interactions between neural, vascular and epithelial components of the esophagus. *J Physiol Pharmacol* 66: 415–420, 2015.
44. **Schenck K, Schreurs O, Hayashi K, Helgeland K.** The role of nerve growth factor (NGF) and its precursor forms in oral wound healing. *Int J Mol Sci* 18: E386, 2017. doi:10.3390/ijms18020386.
45. **Shabbir A, Cox A, Rodriguez-Menocal L, Salgado M, Van Badiavas E.** Mesenchymal stem cell exosomes induce proliferation and migration of normal and chronic wound fibroblasts, and enhance angiogenesis in vitro. *Stem Cells Dev* 24: 1635–1647, 2015. doi:10.1089/scd.2014.0316.
46. **Shaw TJ, Martin P.** Wound repair: a showcase for cell plasticity and migration. *Curr Opin Cell Biol* 42: 29–37, 2016. doi:10.1016/j.ceb.2016.04.001.
47. **Shvartsman D, Storrie-White H, Lee K, Kearney C, Brudno Y, Ho N, Cezar C, McCann C, Anderson E, Koullias J, Tapia JC, Vandenburgh H, Lichtman JW, Mooney DJ.** Sustained delivery of VEGF maintains innervation and promotes reperfusion in ischemic skeletal muscles via NGF/GDNF signaling. *Mol Ther* 22: 1243–1253, 2014. doi:10.1038/mt.2014.76.
48. **Sivilia S, Paradisi M, D'Intino G, Fernandez M, Pirondi S, Lorenzini L, Calzà L.** Skin homeostasis during inflammation: a role for nerve growth factor. *Histol Histopathol* 23: 1–10, 2008. doi:10.14670/HH-23.1.
49. **Song H, Wu F, Zhang Y, Zhang Y, Wang F, Jiang M, Wang Z, Zhang M, Li S, Yang L, Wang XL, Cui T, Tang D.** Irisin promotes human umbilical vein endothelial cell proliferation through the ERK signaling pathway and partly suppresses high glucose-induced apoptosis. *PLoS One* 9: e110273, 2014. doi:10.1371/journal.pone.0110273.
50. **Steinle JJ, Granger HJ.** Nerve growth factor regulates human choroidal, but not retinal, endothelial cell migration and proliferation. *Auton Neurosci* 108: 57–62, 2003. doi:10.1016/S1566-0702(03)00151-6.
51. **Stoeckel K, Thoenen H.** Retrograde axonal transport of nerve growth factor: specificity and biological importance. *Brain Res* 85: 337–341, 1975. doi:10.1016/0006-8993(75)90092-X.
52. **Takano S, Uchida K, Miyagi M, Inoue G, Fujimaki H, Aikawa J, Iwase D, Minatani A, Iwabuchi K, Takaso M.** Nerve growth factor regulation by TNF-α and IL-1β in synovial macrophages and fibroblasts in osteoarthritic mice. *J Immunol Res* 2016: 5706359, 2016. doi:10.1155/2016/5706359.
53. **Tiaka EK, Papanas N, Manolakis AC, Maltezos E.** The role of nerve growth factor in the prophylaxis and treatment of diabetic foot ulcers. *Int J Burns Trauma* 1: 68–76, 2011.
54. **Troullinaki M, Alexaki VI, Mitroulis I, Witt A, Klotzsche-von Ameln A, Chung KJ, Chavakis T, Economopoulou M.** Nerve growth factor regulates endothelial cell survival and pathological retinal angiogenesis. *J Cell Mol Med* 23: 2362–2371, 2019. doi:10.1111/jcmm.14002.
55. **Truzzi F, Marconi A, Pincelli C.** Neurotrophins in healthy and diseased skin. *Dermatoendocrinol* 3: 32–36, 2011. doi:10.4161/derm.3.1.14661.
56. **Tsuneki H, Sekizaki N, Suzuki T, Kobayashi S, Wada T, Okamoto T, Kimura I, Sasaoka T.** Coenzyme Q10 prevents high glucose-induced oxidative stress in human umbilical vein endothelial cells. *Eur J Pharmacol* 566: 1–10, 2007. doi:10.1016/j.ejphar.2007.03.006.
57. **Wang J, He C, Zhou T, Huang Z, Zhou L, Liu X.** NGF increases VEGF expression and promotes cell proliferation via ERK1/2 and AKT signaling in Müller cells. *Mol Vis* 22: 254–263, 2016.
58. **Zhang M, Zhang Y, Ding J, Li X, Zang C, Yin S, Ma J, Wang Y, Cao Y.** The role of TrkA in the promoting wounding-healing effect of CD271 on epidermal stem cells. *Arch Dermatol Res* 310: 737–750, 2018. doi:10.1007/s00403-018-1863-3.